Minimizing Filtering With Ripple Steering

A Practical Approach For Transition-Mode PFC Pre-Regulators

by Claudio Adragna, STMicroelectronics

A major limitation of Transition-Mode (TM) PFC pre-regulators is their considerable input ripple current, requiring a large differential mode (DM) line filter to meet EMI requirements. The ripple-steering technique, with its ability to reduce an inductor ripple current -- theoretically to zero -- can be very helpful in reducing the need for DM filtering in any offline switching converter, and in PFC pre-regulators in particular, where DM noise is an issue because there is no electrolytic capacitor just after the bridge. This technique is illustrated here, providing both the necessary theoretical base and practical considerations to enable a successful implementation.

Coupled magnetic devices have been with us since the early days of Electronics, and their application to power switching circuits dates back to the late 70s with the experiments on the Ćuk converter, from which originated "magnetic integration." With this technique inductors and transformers are combined into a single physical structure to reduce component count, usually with little or no penalty at all on the converter's characteristics, sometimes even enhancing its operation.

During Dr Ćuk's experiments on the converter named after him, the zero-ripple current phenomenon was first observed. The technique derived by the use of this phenomenon is known as ripple-steering or ripple cancellation. Despite its usefulness, it has not, until now, had the broad success it certainly deserves. Reference [1], besides providing an excellent discussion, gives an interesting historical outline of the subject and a comprehensive bibliography as well.

The application of the zero-ripple current phenomenon is of considerable interest in switching converters, where there are at least two reasons why it is desirable to minimize inductor ripple currents. First, it reduces the stress on converter capacitors, resulting in either lower associated power loss or more relaxed filtering requirements. Second, and often more important, most converter topologies have pulsating current at either input or output, or both, and most applications require low conducted noise at both ports for EMC or load requirements.

This issue is commonly addressed with the use of additional LC filters, whose impact on both the overall converter size and cost is not at all negligible, not to mention that sometimes there can even be stability issues if the design is not carefully carried out. In offline converters, where EMC regulations specify limits to the amount of conducted and radiated emissions, a technique like ripple-steering that makes the input current non-pulsating, or nearly so, can be particularly advantageous. Since it eliminates most of the differential-mode conducted noise, it enables the reduction in EMI filter size and complexity, especially in its differential filtering section (Cx capacitors and differential mode inductors).

Reducing Cx capacitors to a minimum brings an additional benefit to applications with tight specifications on standby consumption: Cx capacitors cause a considerable reactive current to flow through the filter, which is a source of additional and unwanted loss (even 0.1 W or more at high line voltages); further, the discharge resistor that must be placed in parallel to Cx for safety can be higher. As a result, both losses will be minimized.

Among offline converters, PFC boost pre-regulators are those that pose the most serious issues of EMI filtering: although their input currents are not chopped, minimizing high-frequency harmonics,

they are devoid of the electrolytic bulk capacitor just after the bridge rectifier, effectively bypassing a large amount of differential-mode noise and their EMI filters need a bigger DF section.

Fortunately, among converter topologies, boost is also one where ripple-steering can be easily implemented. It is not as easy as with Ćuk and SEPIC converters, which already have two inductors that can be coupled on a common magnetic core; however, on a complexity scale, boost and buck converters come next, with their single-winding inductor and with the absence of isolation issues.

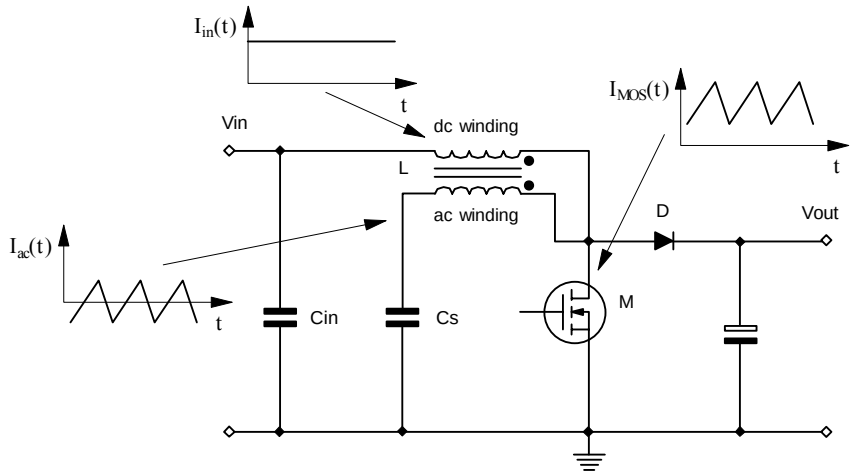

Fig. 1: Modification Of Boost Topology To Achieve Zero-Ripple Input Current

Fig. 1 shows a boost converter modified to achieve zero-ripple inductor current and have non-pulsating input current. A second winding has been added to the boost inductor, with the driven end (that connected to the MOSFET) in common, and a capacitor Cs (the smoothing capacitor). There is a dc path between Cs and the input of the converter, thus the voltage on Cs equals Vin. This is essential in order for the additional winding (termed ac or cancellation winding) to be able to divert, or steer, the ac component (ripple current) from the externally accessible dc winding: the voltage across them must be the same all the time.

After reviewing the theory, we will consider the realization of zero-ripple inductor current in a TM PFC pre-regulator, whose large input ripple is one of the major limitations to use at higher powers.

Zero-Ripple Current Phenomenon: The Theory

From an electrical standpoint a system of two coupled inductors is a linear, time-independent, two-port circuit which, neglecting losses, is described by the following branch-constitutive equations:

$$\begin{vmatrix} v_1(t) \\ v_2(t) \end{vmatrix} = \begin{vmatrix} L_1 & M \\ M & L_2 \end{vmatrix} \frac{d}{dt} \begin{vmatrix} i_1(t) \\ i_2(t) \end{vmatrix} \qquad (1)$$

where, L_1 and L_2 are the self-inductances of the inductors and M their mutual inductance. The mutual inductance is linked to the self-inductances by the relationship:

$$M = k\sqrt{L_1 L_2} \qquad (2)$$

where, k, which lies in the range $0 \le k \le 1$, is the so-called coupling coefficient and is a measure of the degree of magnetic coupling between the inductors. Physically, they will be made up of two windings, composed of N_1 and N_2 turns respectively, wound on the same core of magnetic material.

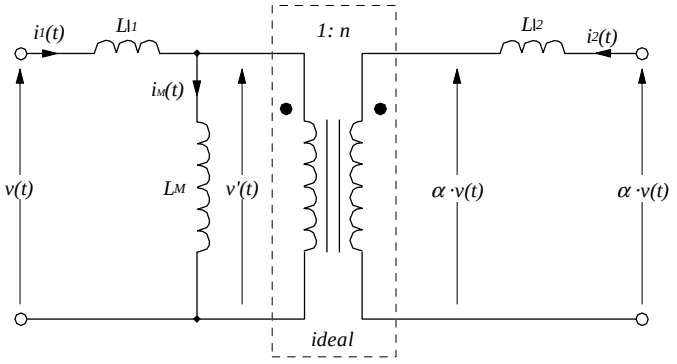

Fig. 2: Coupled Inductor Model And Zero-Ripple Secondary Current Conditions

Consider the coupled inductor model shown in Fig. 2, excited by proportional terminal voltages $v(t)$ and $\alpha v(t)$ (α = constant). LI_1 and LI_2 are the primary and secondary leakage inductance respectively, L_M the primary magnetizing (mutual) inductance, and n the physical turns ratio N_2/N_1. As a reminder, the following relationships hold between the parameters of the equivalent circuit of Fig. 2 and the ones in the branch-constitutive equations (1):

$$\begin{cases} L_M = \dfrac{M}{n} \\ L_{\ell 1} = L_1 - L_M = L_1 - \dfrac{M}{n} \\ L_{\ell 2} = L_2 - n^2 L_M = L_2 - nM \end{cases} \qquad (3)$$

In order for the ripple current $i_2(t)$ to be zero, the voltage across the secondary leakage LI_2 must be zero, that is the voltage on either side of LI_2 must be equal to one another. The voltage applied to the left-hand side of LI_2 will be equal to $nv'(t)$. If $i_2(t) = 0$ the voltage impressed on the primary side of the ideal transformer $v'(t)$ will be given by the ratio of the inductive divider composed of the primary leakage inductance LI_1 and the magnetizing inductance L_M. Then, there will be zero-ripple current on the secondary side of the coupled inductor if the following condition is fulfilled:

$$n\,v'(t) = \alpha v(t) \;\Rightarrow\; n\frac{L_M}{L_{\ell 1}+L_M} v(t) = \alpha v(t) \;\Rightarrow\; \frac{L_M}{L_{\ell 1}+L_M} n = \frac{L_M}{L_1} n = \alpha, \qquad (4)$$

This equation also provides a physical interpretation of the zero-ripple current phenomenon: it occurs when the turns ratio exactly compensates for the primary winding leakage flux, so that the primary winding induces, by transformer effect, a voltage identical to the excitation voltage applied to the secondary winding.

With the same technique it is possible to find the condition for zero-ripple primary current (just reflect the magnetizing inductance L_M to the secondary side); the result is:

$$\alpha v(t) \frac{n^2 L_M}{L_{\ell 2}+n^2 L_M} \frac{1}{n} = v(t) \;\Rightarrow\; \frac{n L_M}{L_{\ell 2}+n^2 L_M} = \frac{L_M}{L_2} n = \frac{1}{\alpha}$$

Most commonly, and this also holds true for the modified boost converter (Fig. 1, again), the two windings "see" the same voltage (α=1), hence this will be the case that will be further considered. Therefore:

$\dfrac{L_M}{L_1} n = 1$ condition for zero-ripple secondary current,

$\dfrac{L_M}{L_2} n = 1$ condition for zero-ripple primary current.

Note that ripple current cannot be reduced to zero in both windings simultaneously. With the aid of Fig. 2 also note that the value of the inductance of the winding with zero-ripple current is irrelevant as only dc current can flow. Consequently, the zero-ripple current winding reflects an open circuit to the other winding and the inductance seen at its terminals exactly equals its self-inductance.

The designation of which winding is the primary or the secondary is only a convention. Therefore, we will consider only one zero-ripple current condition and arbitrarily assume the condition to be assigned to the secondary winding:

$$\frac{L_M}{L_1} n = 1. \qquad (5)$$

Consistent with the terminology used for the boost converter (Fig. 1) the secondary winding will be termed the "dc" winding, while the primary winding will be termed the "ac" or "cancellation" winding. Eq. (5) can be written in different ways that can be deduced considering Eqs. (2) and (3):

$$\frac{L_M}{L_1} n = \frac{M}{L_1} = k\sqrt{\frac{L_2}{L_1}} = 1 \qquad (6),$$

and that can be useful for some of the considerations that follow.

Sensitivity Of Zero-Ripple Current Condition

In the real world of coupled inductors it is unthinkable to reduce the ripple current in a winding exactly to zero and produce a perfect ripple steering. There are two basic reasons for this:

- *Zero-ripple condition mismatch.* In practice, the inductance of a winding is determined by the number of turns and the average permeability of the associated magnetic circuit. The turns ratio can assume only discrete values (ratio of two integer numbers) and it is difficult to control the average permeability to achieve the exact value that meets condition (5). Even if this may be obtained in occasional samples, manufacturing tolerances cause the actual value to deviate from the target in mass production.
- *Impressed voltage mismatch.* In reality there are several factors that cause the two windings to be excited by voltages that are not exactly equal to one another. There are internal factors, such as the voltage drop across the winding resistance (neglected so far), and external factors, such as the finite capacitance value of the smoothing capacitor C_S and its ESR.

To evaluate the residual ripple current it is convenient to use the model of Fig. 2. Based on that, after some algebraic manipulations, it is possible to write:

$$\frac{di_2(t)}{dt} = \frac{v_2(t) - k\sqrt{\frac{L_2}{L_1}} v_1(t)}{L_2\left(1-k^2\right)} \qquad (7),$$

which can be re-written as:

$$\frac{di_2(t)}{dt} = \frac{1}{L_2\left(1-k^2\right)} \left[\underbrace{v_2(t) - v_1(t)}_{\substack{\text{Impressed voltage} \\ \text{mismatch}}} + \underbrace{\left(1 - k\sqrt{\frac{L_2}{L_1}}\right) v_1(t)}_{\substack{\text{Zero ripple condition} \\ \text{mismatch}}} \right] \qquad (8)$$

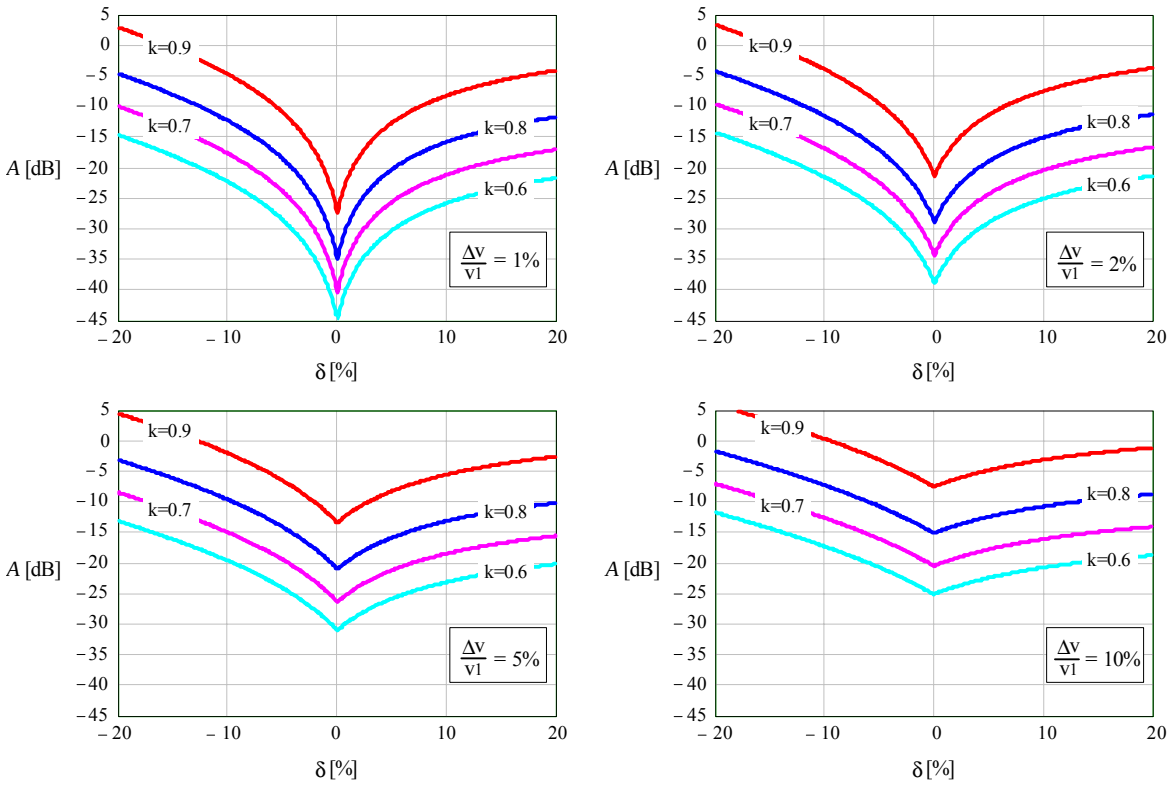

Fig. 3: Ripple-Current Attenuation Vs. Error Sources For Various Winding Couplings

Although the inductance of the dc winding is theoretically irrelevant to the phenomenon itself (the inductance could even be zero), Eqs. (7) and (8) show that in practice this inductance is significant because it determines the actual residual ripple current resulting from the unavoidable mismatches. More precisely, these equations highlight the need for a high-leakage magnetic structure, so that a low coupling coefficient k maximizes the residual inductance $L_2 (1 - k^2)$.

With the aid of either Eq. (7) or (8) it is possible to evaluate the attenuation *A*, defined as the ratio of the residual ripple $di_2(t) / dt$ to the ripple that would be there without the coupled inductor. The result of this analysis is shown in Fig. 3, where *A* is plotted for different values of the relative voltage mismatch $\Delta v(t) / v_1(t)$ and of the coupling coefficient k, as a function of the zero-ripple condition mismatch δ.

From the inspection of these plots it is apparent that a low coupling coefficient is essential for a good attenuation even if the zero-ripple condition is not exactly met. For example, to achieve attenuations always greater than 15 dB even with a tolerance of ±10% on the value of δ and 5% voltage mismatch, the coupling coefficient k must be 0.7 or lower. However, using very low k values involves more turns for the dc winding, which could be an issue in inductor construction.

Note that in case of under-compensation ($\delta < 0$) the residual ripple can be higher than the original value: this is due to a too low value of the residual inductance $L_2 (1 - k^2)$.

Zero-Ripple Current Phenomenon: The Practice

Before going into details of the practical realization of a coupled inductor able to provide ripple steering, it is useful to draw some conclusions of considerable practical interest from the theoretical analysis carried out in the previous sections:

- Essentially, to achieve zero-ripple current in a coupled inductor with low sensitivity to parameter spread, a high-leakage magnetic structure is needed, which is contrary to the traditional design practice. So considering inductors realized with a "gapped-ferrite core plus bobbin" assembly, the usual concentric winding arrangement is not recommended, although a higher leakage inductance can be achieved by spacing the windings apart. However, it is difficult to obtain a repeatable value because it depends on values (such as winding surface irregularities or spacer thickness) difficult to control. Other methods, such as placing the windings on separate core legs, or side-by-side on the same leg (see Fig. 4), permit much better controlled leakage-inductance values, as they are related to the geometry of the bobbin. Slotted bobbins like (see Fig. 5) allow side-by-side winding arrangements; they are quite commonly available so they will be considered here.

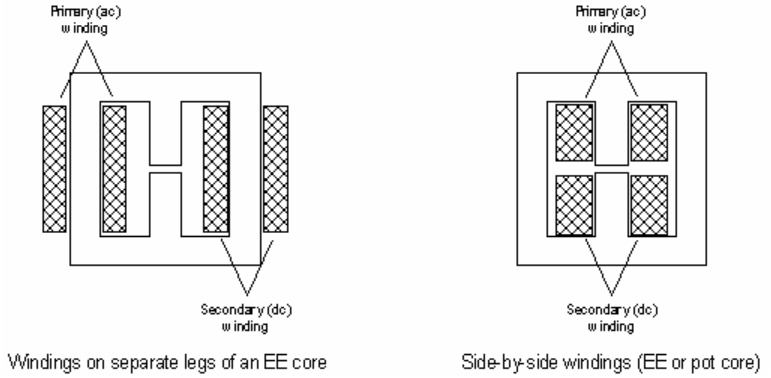

Fig. 4: Examples Of High-Leakage Magnetic Structures (Cross-Section)

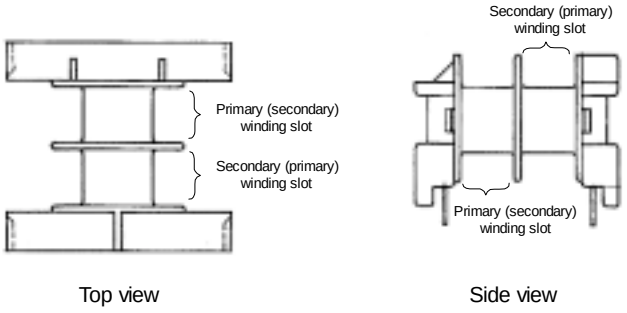

Fig. 5: Two-Section Slotted Bobbin Suggested For Realizing The Coupled Inductor

The fundamental action of the smoothing transformer is to split up the current into its dc component, flowing in one winding, and its ac component, flowing in the other one. The total rms current in the windings is unchanged; hence the total copper area needed to handle the two currents separately will be quite close to that of a single inductor carrying the total current. However, the slots are typically equal to one another, whereas the dc and ac currents are not. As compared to a single inductor, no core size increase is typically expected because of insufficient winding window area, except for a few marginal cases where the uneven current splitting and the slight decrease of window area due to slotting becomes critical. An additional important point is that the dc winding

can be made with a single wire, since its residual ac current is low; only the ac winding will be made with Litz or multi-stranded wire. This minimizes the cost of the extra winding.

The same splitting of current occurs to magnetic flux as well: the ac and the dc components are generated separately but the total flux will be the same as in a single inductor. So no core size increase is expected because of flux density limitations (core saturation) or core loss. Also the core size selection approach will be the same.

To complete the picture, an important property of the "gapped-ferrite core plus bobbin" assembly should be recalled. The reluctance of the leakage flux path is constant for a given core geometry and is independent of the gap thickness, l_{gap}: essentially, it is a function of the physical dimensions of the core and the distance between the windings. This implies that the leakage inductance of the primary winding, L_{l1}, depends only on the turns number N_1 and will not change if l_{gap} is adjusted. However, the total primary inductance $L_1 = L_{l1} + L_M$ is strongly affected by the gap thickness, but it is only the magnetizing inductance L_M that changes. With reference to the zero-ripple current condition (5):

$$\frac{L_M}{L_1} n = \frac{L_1 - L_{\ell 1}}{L_1} n = 1,$$

once the core and the associated bobbin are defined, it is possible to control L_{l1} and L_M separately, acting on N_1 and l_{gap} respectively; the turns number N_2 will be chosen so that the ratio $n = N_2/N_1$ fulfills condition (5).

At this point, we have all the elements needed to outline a step-by-step practical design procedure. For the details of Steps 2 to 4, please refer to the algorithm described in Rference [2].

1. Design the PFC stage as with a conventional inductor. In particular, determine the required inductance value L_1, the maximum peak short-circuit current and, considering full load conditions, the rms, dc and ac inductor currents, recalling that between them the following relationship holds:
   $$I_{AC} = \sqrt{I_{RMS}^2 - I_{DC}^2}$$
2. Assuming that an EE-shaped ferrite core with a slotted bobbin will be used, determine the maximum flux density and the maximum flux swing the core will be operated at. Tentatively select a core size and determine the loss limit, both in the winding (P_{Cu}) and the core (P_{Fe}). Calculate the turns number, N_1, of the ac winding in such a way that the desired inductance value L_1 can be obtained without exceeding either the core saturation limits or the permitted core loss. Determine the required gap length.
3. Calculate the conductor size for the ac winding considering that its resistance must be:
   $$R_{ac} \le \frac{P_{Cu}}{2 I_{AC}^2}$$
   To minimize skin and proximity effects, use litz or multi-stranded wire.
4. Calculate the conductor size for the dc winding considering that its resistance must be:
   $$R_{dc} \le \frac{P_{Cu}}{2 I_{DC}^2}$$
   Since dc current will flow through this winding a single wire will be used.
5. Wind the entire ac winding in one slot and fix it. In the other slot wind a couple of layers of the wire that will be used for the dc winding. Temporarily assemble the core set. If the two half-cores are not gapped, use a gap value close to that calculated, to make the next measurements under conditions as close to those of a finished sample as possible. Consider also that small gaps amplify measurement errors.

6. Using any of the methods described in the Appendix, measure the leakage inductance L_{Lk} (referred to the ac winding) obtained in this way and calculate a first-cut value for N_2:

$$N_2 = N_1 \frac{L}{L - L_{LK}},$$

where, in this case, L is the measured inductance of the ac winding. Add 5% to the result, to account for the slight coupling improvement that there will be as the dc winding will be entirely in place, and round up to the next integer. Let the final number be N_2.
7. After removing the layer used for the preliminary measurement and the core, wind the N_2 turns of the dc winding. Do not fix the end of the wire permanently because N_2 should be greater than the value that meets the zero-ripple condition, and some turns will need to be taken out in the following step.
8. Reassemble the core and adjust the air gap so as to get the required value L_1. Measure the leakage and the magnetizing inductances (see the Appendix) and check if Eq. (5) is met. If not, remove one turn and repeat the step until condition (5) is close to being met.
9. Connect the coupled inductor to the converter, power it on and measure the ripple on the dc winding. It should be quite small. If it looks like Fig. 6 (on the left), where the ripple is 180° out-of-phase, there are still too many turns on the dc winding and they should be further reduced. If the ripple looks like Fig. 6 (on the right) the turns of the dc winding have been reduced too much. If it is not possible to re-add turns to the dc winding, either the air gap must be reduced if possible (paying attention to saturation!), or the turns number of the ac winding must be reduced. Also in this case it is possible to fine tune by adjusting the gap, if possible. Only when the ripple has been minimized can one permanently fix the dc winding wire end to the bobbin pin. Record the final values of N_1, N_2 and l_{gap}.

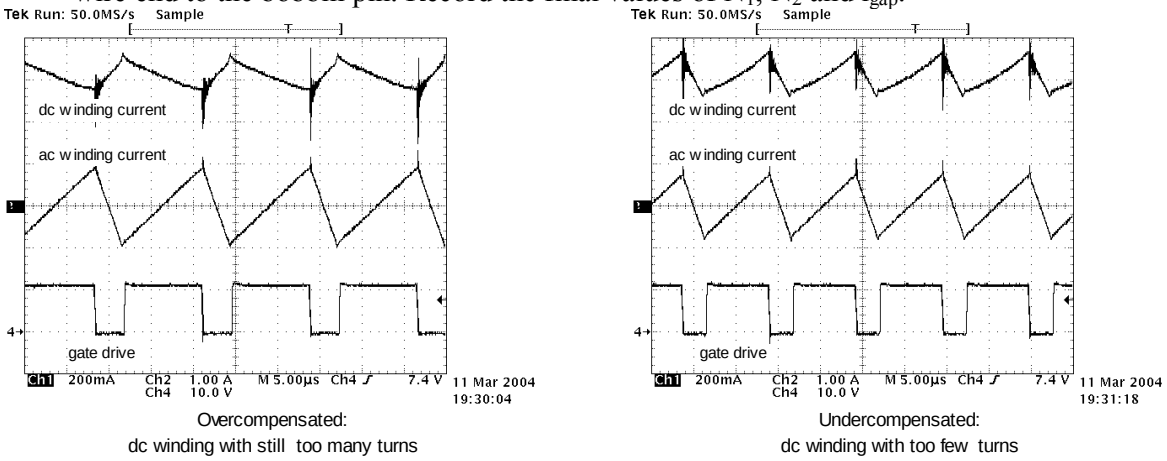

Fig. 6: Partial Ripple Cancellation: Left, Overcompensated; Right Undercompensated

Note that the first four steps of this procedure are the same as those for a conventional inductor. Starting from Step 5, the procedure becomes empirical and quite tricky and might be time-consuming as well. Fortunately, this burden of work needs to be done to make the first prototype only. Take note of the leakage inductance per squared turn that you get, it can be re-used in another design with the same core.

There is still an important practical issue to consider. When the two half cores are assembled, even if they are kept together well, they are typically quite loose inside the bobbin, unless one uses mounting clips or gluing (quite impractical to use during the cut-and-try phase!). The position of the core inside the bobbin, especially along the direction of the legs, is critical because it changes the position of the air gap with respect to the windings. Moving the core causes significant variations of

the magnetizing inductance, thus it is recommended to fix the cores in a stable position as close as possible to that of the finished sample before doing any inductance measurement or test on the converter circuit.

At this point the question is: how much spread can one expect in mass production? Side-by-side winding arrangements in slotted bobbins are quite commonly used when making common-mode chokes and wound component manufacturers have long-standing experience in that. For wires which are not too thin (say, above 0.2 mm) with a good winding machine it is not difficult to have a tolerance around 4 - 5% on the leakage inductance. As for the self-inductance of one winding, using gapped cores the tolerance on the A_L factor (nH/turn^2), deducible from catalogs, is 5% or better for air gaps >0.1mm for small cores (e.g. an E30/15/7) and for air gaps >0.4 mm in case of bigger cores (e.g. an E55/28/21). An additional 3% tolerance has to be typically considered due to the above mentioned displacement of the core inside the bobbin. It is therefore possible to assume 5% tolerance for L_{l1} and 8% tolerance on L_1.

The turns ratio, *n*, is not subject to production spread; the rounding error just introduces a fixed mismatch in the zero-ripple current condition. Again, using gapped cores where the air gap cannot be adjusted to compensate for the mismatch, the rounding error is ≤0.5 turns, hence the maximum absolute error that it introduces on *n* is $\pm 0.5 / N_1$ and the maximum relative error will be $(\pm 0.5 / N_1) / n = \pm 0.5/N_2$.

With some simple algebraic manipulations it is possible to find the relative error on the zero-ripple current condition, Eq. (5), due to the spread δ_{l1} and δ_1 of L_{l1} and L_1 respectively, is:

$$\delta = (n-1)\frac{\delta_1 - \delta_{\ell 1}}{1+\delta_1}$$

Since *n* is slightly greater than 1 the effect of the spread of L_{l1} and L_1 is attenuated. To take an example, with n=1.3, the resulting maximum spread will be δ = -4.2% to +3.6%.

With good approximation, it is possible to consider that this tolerance band is centered on a value shifted by the rounding error. Looking back at Fig. 3, the attenuation factor *A* degrades more quickly for negative δ values, hence it is better to round N_2 to the upper integer, to provide a "positive offset" to δ and be in a region where *A* changes less. To continue the example, if N_2=50 turns (rounded up), the rounding error will be +1%, and the total tolerance band will be -3.2% / +4.6%. With 5% voltage mismatch, *A* will always exceed 20 dB.

Smoothing Capacitor Selection

The capacitance of the smoothing capacitor, Cs, should be as large as possible and its ESR as low as possible to minimize the impressed voltage mismatch. Although this assertion is always true, the usage in a PFC pre-regulator poses an important limitation to the capacitance value that can be used.

The dc path between the capacitor and the input port of the converter (Fig. 1) causes Cs to appear as if directly connected to the input rectifier bridge so it will add to the capacitance normally placed just after the bridge and will contribute in the increase to the THD of the low-frequency line current as well as lowering the PF.

Although the capacitor placed after the bridge can be reduced just because of the ripple-steering, the value of Cs must in any case be selected by trading off the ripple-steering effectiveness against the

need for a low line current THD. The peak-to-peak voltage ripple ΔV appearing across the capacitor, which is essentially twice the voltage mismatch, is related to the ac ripple amplitude ΔI:

$$\Delta v_{pk-pk} = \frac{\Delta I}{8 f_{sw} C_s},$$

which will be maximum at the top of the sinusoid at minimum line voltage, where the amplitude of the ac current is maximum and the switching frequency is close to its minimum value. Substituting the values that can be derived by the PFC relationships, Rference [4], it is possible to find the following expression for the relative voltage mismatch:

$$\left.\frac{\Delta v(t)}{V_1(t)}\right|_{max} = \frac{L_1}{4 C_s}\left(\frac{Pin_{max}}{Vin^2_{min}}\right)^2 \frac{Vout}{Vout - \sqrt{2}\, Vin_{min}}$$

Typically, the values normally used for the capacitor after the bridge (5 - 15 nF/W) lead to a good compromise. Polypropylene capacitors are recommended for their low ESR.

A Ripple-Free Input Current PFC Pre-Regulator

Fig. 7 shows the schematic of a PFC pre-regulator based on the boost topology modified by adding the cancellation winding to the boost inductor and a capacitor as sketched in Fig. 1. Table 1 lists its electrical specification, approximately tailored to that of a typical high-end laptop PC power adapter, while Table 2 gives the details of the modified boost inductor.

The design of the pre-regulator is carried out in exactly the same way as for a traditional stage. The coupled inductor, the crucial element of this application, is built following the previous procedure.

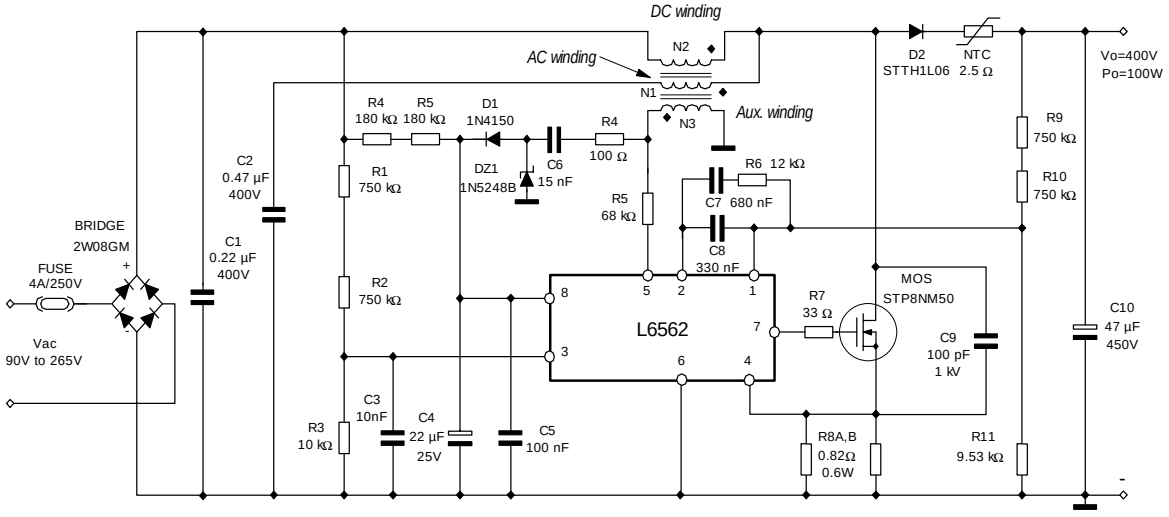

Fig. 7: Schematic Of 100-W PFC Pre-Regulator With Ripple-Free Input Current

The controller chip used is the L6562, Rference [3], from STMicroelectronics, suitable for implementing TM-controlled PFC pre-regulators up to 300 W. A prototype of the pre-regulator has been built and evaluated on the bench. The diagrams of Figs. 8 and 9 show its typical performance; Figs. 10 to 12 show some significant waveforms. The filter shown in Fig. 13, assembled on a separate board, was used to connect the test board to the ac source during the evaluation.

Symbol	Description	Value	Unit
V_{ACmin} - V_{ACmax}	Line Voltage Range	90 - 265	V rms
V_{out}	Regulated Output Voltage	400	V dc
P_{out}	Rated Output Power	100	W
f_{swmin}	Minimum Switching Frequency	50	kHz
H	Expected Minimum Efficiency	90	%
ΔV_{out}	Full-load Output Voltage Ripple	20	V pk-pk
ΔV_{OVP}	Maximum Output Overvoltage	40	V dc

Table 1: 100-W PFC Pre-Regulator With Ripple-Free Input Current: Electrical Specification

Core	E30/15/7, N67 material or equivalent				
Bobbin	2-slot, 10 pins, horizontal mounting				
Air gap	0.9 mm for an ac winding inductance of 400 µH				
Windings Spec & Build	**Winding**	**Pin S/E**	**Wire**	**Turns**	**Notes**
	ac	10/3	20 x 0.1 mm	72	Wound in slot 1
	dc	10/1	0.45 mm	98	Wound in slot 2
	aux	6/5	0.1 mm	11	Evenly spaced, on top of dc winding

Table 2: 100-W PFC Pre-Regulator: Coupled Inductor Specification

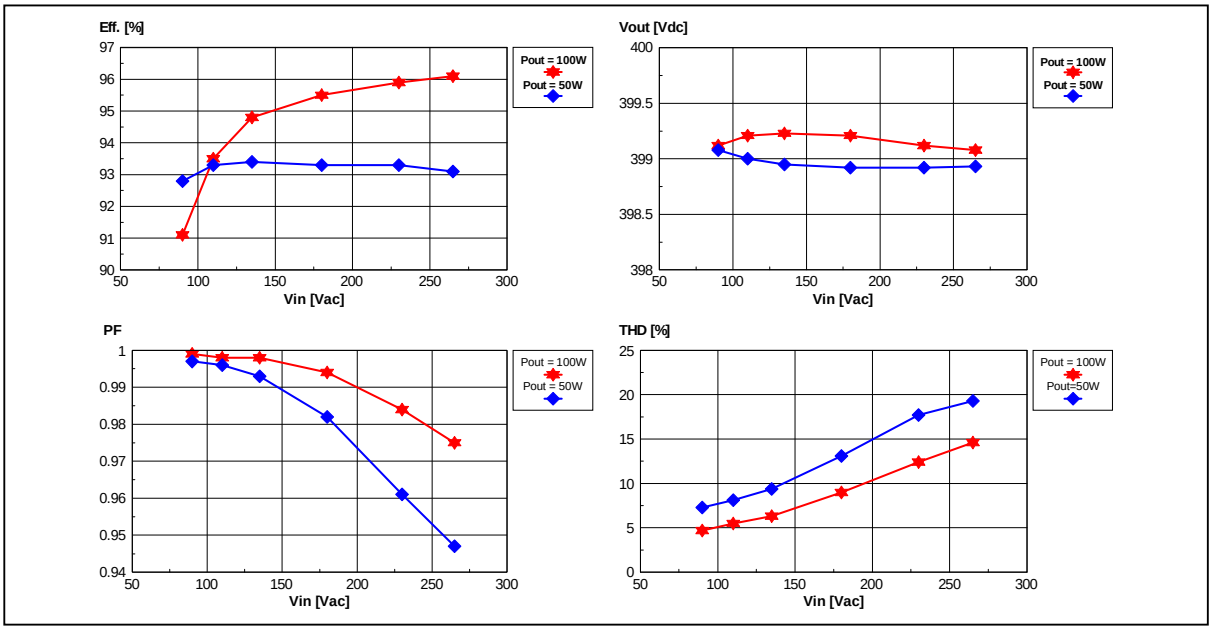

Fig. 8: 100-W PFC Pre-Regulator With Ripple-Free Input Current: Typical Performance

The waveforms of Figs. 10 and 11 are taken at full load, powering the PFC stage from a dc source to get a stable image. On the right, the ac winding and the dc winding current are shown at a comparable vertical scale; on the left the vertical scale of the dc winding current is magnified to emphasize the residual ripple. Note its curvilinear shape resulting from the capacitive voltage ripple across the smoothing capacitor, C2.

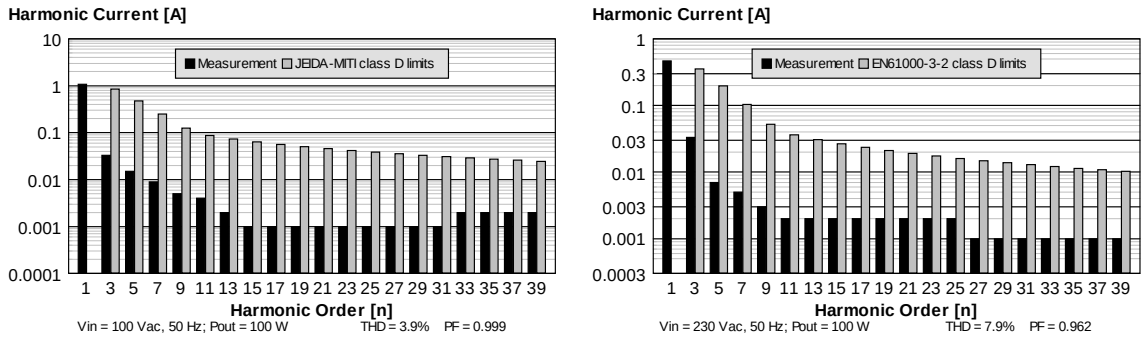

Fig. 9: Harmonic Emissions And Conformity To JEIDA-MITI & EN61000-3-2 Sstandards

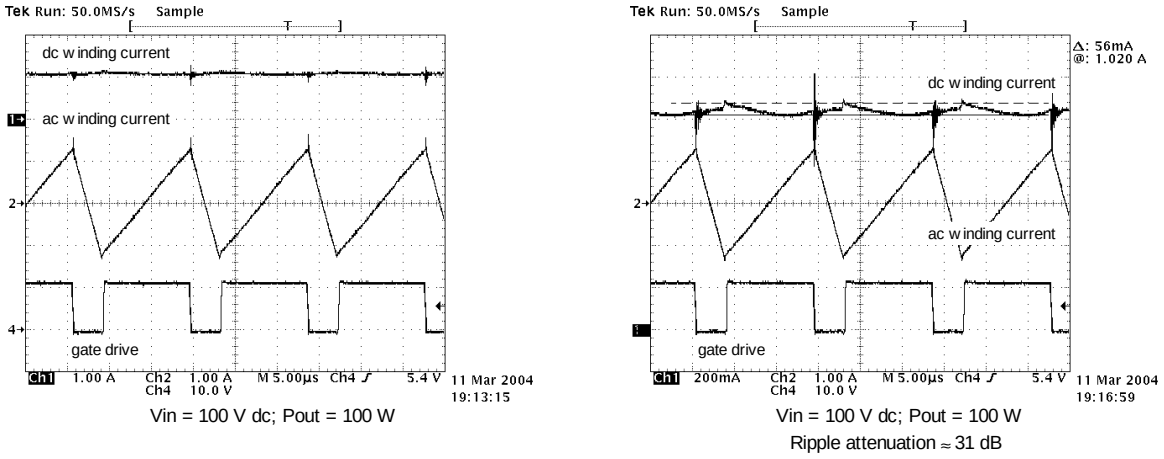

Fig. 10: Winding Currents: Vin = 100 Vdc (Left); Zoomed dc Winding Current (Right)

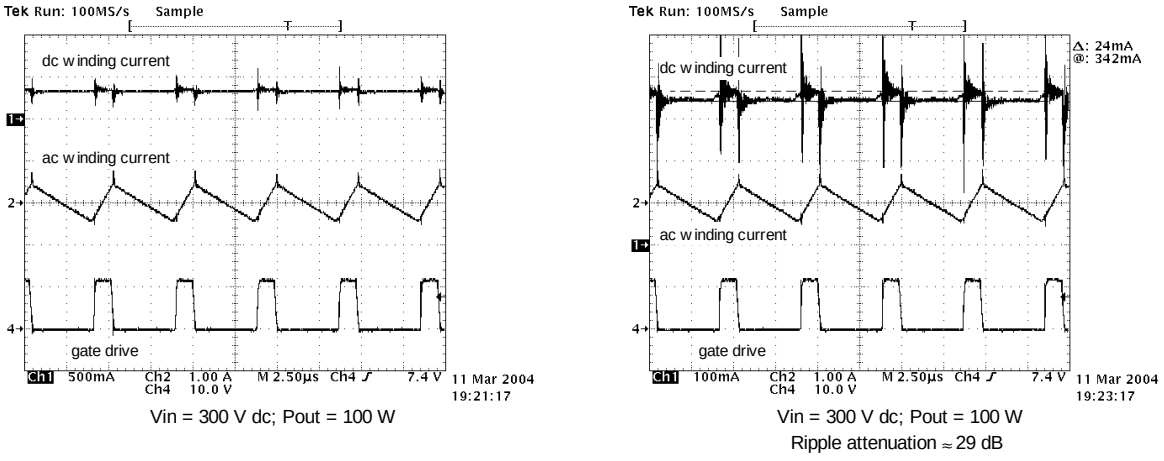

Fig.ure 11: Winding Currents: Vin = 300 Vdc (Left); Zoomed Dc Winding Current (Right)

Fig. 12 shows the effect of the cancellation winding on the input current of the PFC stage with no filter connected to the input: on the left the ac winding is disconnected and the converter operates like a conventional boost; on the right the ac winding has been reconnected.

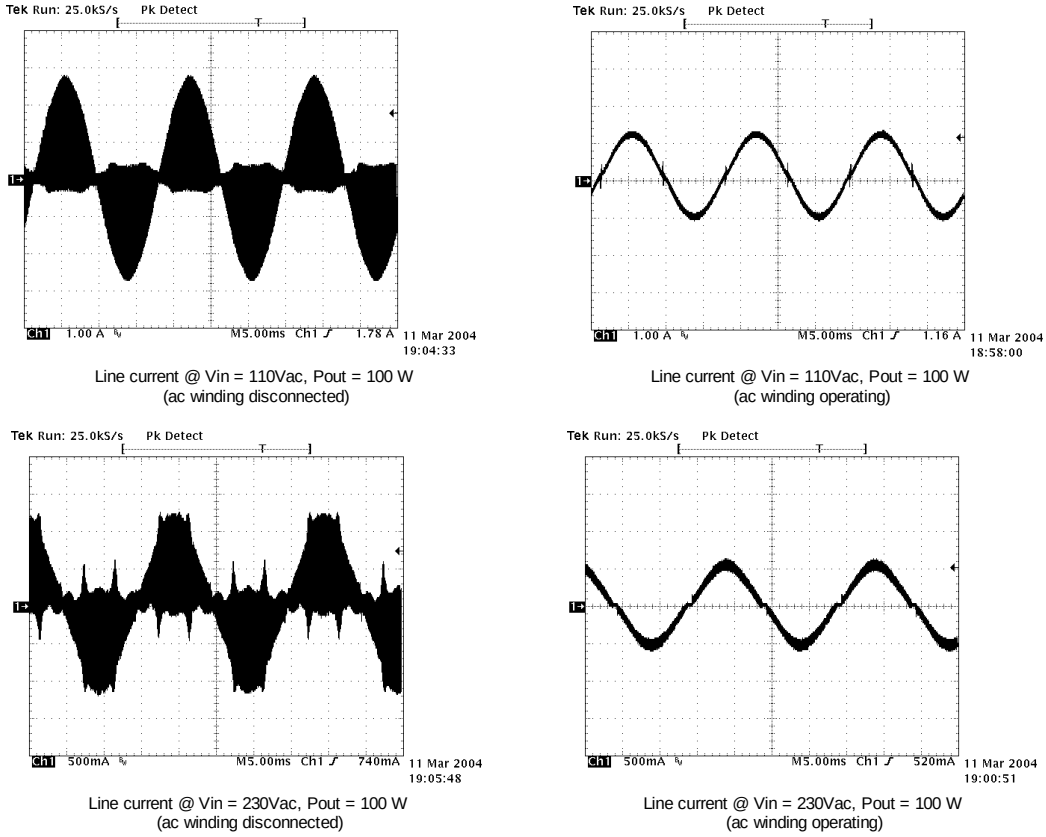

Fig. 12: Effect Of Ac Winding On Line Current Ripple (No LC Filter At Input)

The filter of Fig. 13 was used to perform an EMI pre-compliance test with the aim of evaluating the practical impact of the ripple steering technique on the design of the input EMI filter, by comparing the emissions with and without the ac winding. The results are shown in Figs. 14 and 15.

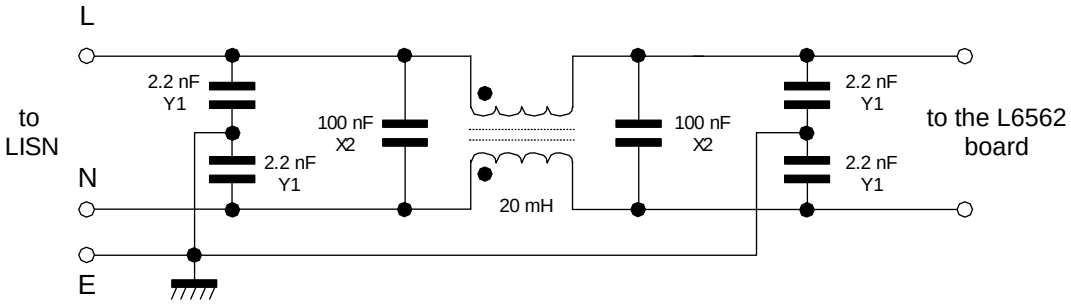

Fig. 13: EMI Filter Used For Efficiency/Harmonic Emissions/Conducted EMI Measurements

The effect of ripple steering is particularly conspicuous up to about 2 MHz, with more than 20 dB attenuation provided. For higher frequencies, where common-mode noise is dominant, its effect becomes negligible and emissions must be controlled with the usual noise control techniques. The emission level with peak detection is well below the quasi-peak and average limits envisaged by the

EN50022 class B, except for the high frequency range (>10 MHz), where the poor assembly plays a crucial role. Thus it is reasonable to expect that with the filter (Fig. 13) assembled on the same PCB it would be fully compliant.

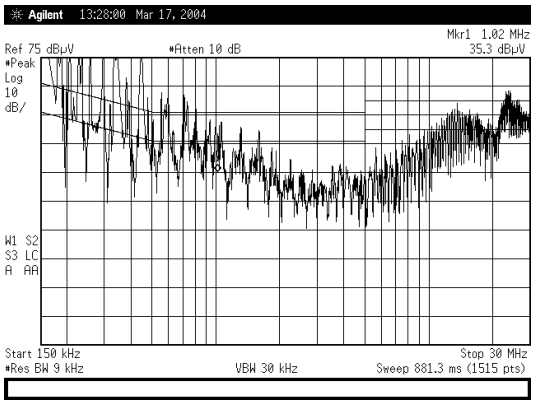

Conducted EMI, peak detection @ Vin = 110Vac, Pout = 100 W
(ac winding disconnected)

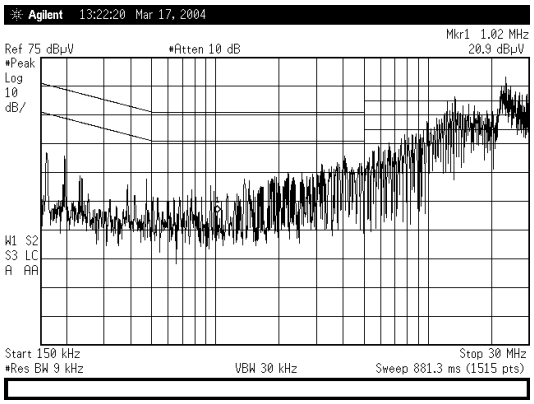

Conducted EMI, peak detection @ Vin = 110Vac, Pout = 100 W
(ac winding operating)

Fig. 14: Conducted EMI: Vin = 110 Vac, Pout = 100 W. Limits: EN50022 class B

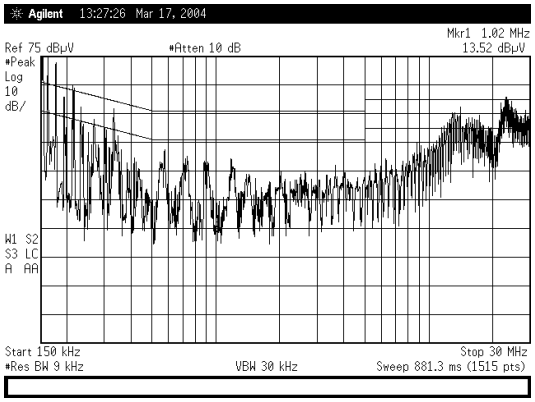

Conducted EMI, peak detection @ Vin = 230Vac, Pout = 100 W
(ac winding disconnected)

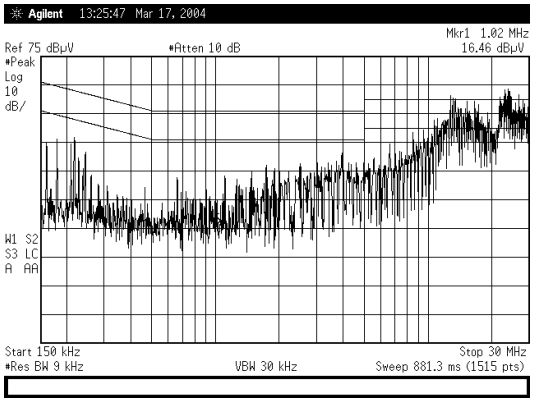

Conducted EMI, peak detection @ Vin = 230Vac, Pout = 100 W
(ac winding operating)

Fig. 15: Conducted EMI: Vin = 230 Vac, Pout = 100 W. Limits: EN50022 class B

To complete the picture, another series of EMI tests was performed to find an input LC filter able to control emissions, without ripple-steering, comparable to that from the filter with ripple-steering (at least in the 150 kHz – 2 MHz band). With the filter shown in Fig. 17 the results (see Fig. 16) look quite similar to those of figures 14 and 15 on the right.

To achieve comparable results a two-cell filter and much larger Cx capacitors (2 x 220 nF + 470 nF against 2 x 100 nF) have been used. Additionally the filter capacitor after the bridge has been increased from 220 nF to 680 nF. This filter is considerably more expensive and deteriorates the overall performance. The full-load efficiency decreases (-1.3% @ 90 Vac, -0.7% @ 230Vac) because of the increased conduction losses in the additional inductor; the no-load losses will be higher because of the larger current circulating through the X caps, the PF and the THD degrade much more rapidly at high line voltage and light load because of the larger X caps and the larger capacitor after the bridge rectifier.

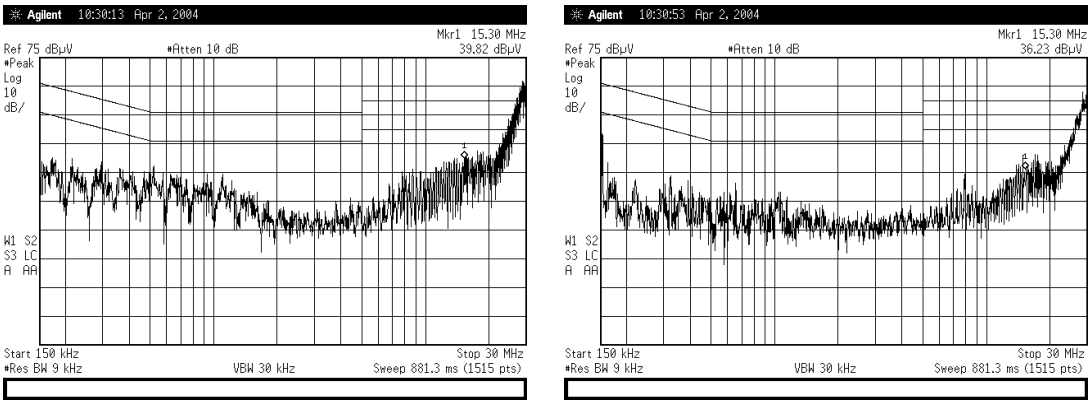

Conducted EMI, peak detection @ Vin = 110Vac, Pout = 100 W
(ac winding disconnected, filter of figure 20)

Conducted EMI, peak detection @ Vin = 230Vac, Pout = 100 W
(ac winding disconnected, filter of figure 20)

Fig. 16: Conducted EMI: Pout = 100 W Without Ripple Steering, With The Filter Of Fig. 17

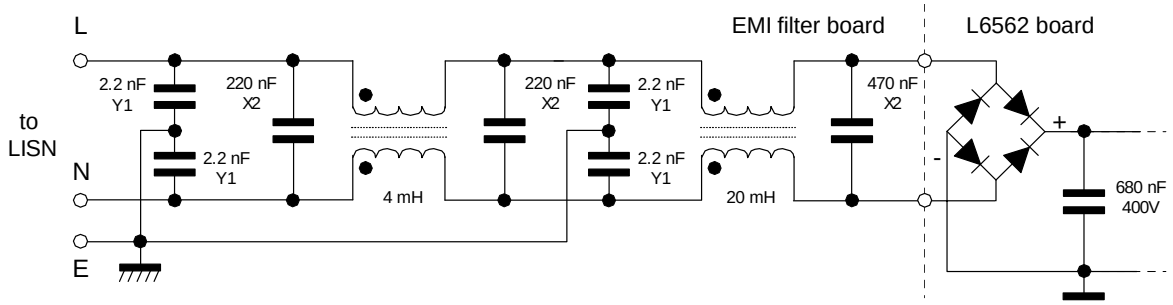

Fig. 17: EMI Filter Used To Achieve The Conducted Emissions In Fig. 16

Conclusions

The ripple-steering technique, with its ability to reduce an inductor ripple current theoretically to zero, has been discussed and the theory outlined. The construction of a coupled inductor has been addressed and a practical design guide given to enable its successful implementation.

A practical application of the ripple-steering technique has been shown: it refers to a TM-controlled PFC pre-regulator where the technique has been used to minimize the input ripple current, which is a major limitation to the use of this simple and efficient topology at higher power levels.

The experimental results have shown that the ripple-steering technique is very effective in reducing the input ripple current and that considerable savings can be achieved in the differential-mode input EMI filter, with the positive side-effect of minimizing the loss due to the filter itself.

References

[1] Hamill, D.C.; Krein, P.T. “A ‘Zero’ Ripple Technique Applicable to Any DC Converter”, Power Electronics Specialists Conference, 1999. PESC 99. 30th Annual IEEE (1999 Volume 2)
[2] “Inductor and Flyback Transformer Design”, Unitrode Magnetics Design Handbook (MAG100A), Section 5
[3] “L6562, Transition-mode PFC controller”, Datasheet
[4] “L6561, Enhanced Transition-mode Power Factor Corrector”, AN966

Appendix: Measuring Coupled Inductor Parameters

From a practical point of view there is the need to measure the parameters of a two-winding coupled inductor L_1, L_2 and M or, equivalently, k and derive those of the equivalent circuit of Fig.2.

L_1 and L_2 are directly measurable. To determine M or k appropriate measurements need to be done, and the best way to proceed is to use a Z-meter, taking the measurements at a low-enough frequency that the parasitic capacitance of the windings can be neglected. There are two basic methods: the open/short-circuit inductance (OS) method and the series-aiding/opposing inductance (AO) method.

With the OS method, three measurements will be taken:

1. The primary inductance with the secondary open (L_1)
2. The primary inductance with the secondary shorted (L_{1s})
3. The secondary inductance with the primary open (L_2)

From Eq. (1), letting $v_2(t)=0$, it is very easy to derive the relationship between the coupling coefficient and the L_{1s} measurement:

$$L_{1s} = L_1 - \frac{M^2}{L_2} = L_1\left(1-k^2\right) \quad \Rightarrow \quad k = \sqrt{1-\frac{L_{1s}}{L_1}}$$

M is obviously:

$$M = k\sqrt{L_1 L_2}$$

Measuring L_{1s} accurately might be an issue, thus this method is suitable when k is close to unity ($L_{1s} << L_1$). It is not recommended when the winding resistance is not negligible.

The AO method is based on the fact that by connecting the two windings in series their combined inductance is given by $L_1 + L_2 \pm 2M$, where the sign given to 2M depends on the way the windings are connected, as shown in Fig. A1. The difference of the two values is thereby equal to 4M.

According to the AO method, four measurements will be taken:

1. The primary inductance with the secondary open (L_1)
2. The secondary inductance with the primary open (L_2)
3. The combined inductance with series-aiding connection (L_A)
4. The combined inductance with series-opposing connection (L_O)

$L_A = L_1 + L_2 + 2M$ $\qquad$ $L_O = L_1 + L_2 - 2M$

Fig. A1: Winding connections: Aiding Flux (Left); Opposing Flux (Right)

It is always $L_A > L_O$, thus, as said before:

$$M = \frac{L_A - L_O}{4} \quad \Rightarrow \quad k = \frac{L_A - L_O}{4\sqrt{L_1 L_2}}$$

The advantage of this method is its low sensitivity to winding resistance and to the impedance of the wire used for connecting the windings. It is not recommended for low values of k because in those cases it would be given by the difference of two similar quantities, and the error might be high.

Whichever method has been used, the parameters of the equivalent circuit of Fig. 2 can be readily calculated from Eq. (3).

About The Author

Claudio Adragna is Application Segment Manager with STMicroelectronics' Telecommunication and Pheripherals/Automotive Groups in Agrate Brianza, Italy. He holds a Laurea (equivalent to a US MS degree) in Electronics Engineering and has been with STM since 1992. Claudio's current responsibilities are for ac-dc power conversion, PWM controllers, PFC controllers, resonant controllers and other ancillary functions. He has previous experience in dc-dc converters, lighting and industrial control Ics and has been published in conference proceedings and specialized magazines. Claudio has numerous application notes posted on the STM website and holds 6 US patents.

as published in...
analog ZONE